CHEMISTRY OF MATERIALS

Communication

pubs.acs.org/cm

Charge Transfer and Fractional Bonds in Stoichiometric Boron Carbide

Swastik Mondal*

CSIR-Central Glass and Ceramic Research Institute, Jadavpur, Kolkata 700032, India

Supporting Information

Boron carbide is one of the most versatile materials of current technological importance.[1−3] Low costs of synthesis combined with many useful properties, such as extreme hardness, photocatalytic activity, a high Hugoniot elastic limit, thermoelectricity, *p*-type semiconducting behavior, paramagnetism and high thermal and chemical stability have made boron carbide a preferred material for a variety of technological applications.[1−7] Despite decades of intense research, the origin of such diverse properties in boron carbide has not yet been fully understood.[1,2] The major challenge to explain the chemical and physical properties of boron carbide in terms of its crystal structure and chemical bonding has remained an unsolved puzzle.[2]

Boron carbide crystallizes in the αR-boron[8] structure type (Figure 1a,b) with $R\bar{3}m$ symmetry, and has the remarkable power to maintain the same general structure through a large variation of atomic proportions.[1−3] Single-crystal X-ray diffraction studies[9−11] have shown that the structure of boron carbide with composition $B_{13}C_2$ consists of icosahedral B_{12} clusters and linear CBC chains. The icosahedral unit comprises two crystallographically independent boron atoms, denoted as B_{Polar} and $B_{Equatorial}$ (henceforth, B_P and B_E). The central boron atom of the CBC chain is denoted as B_{Chain} (henceforth B_C). The B_P atoms of the B_{12} cluster participate in the intercluster B_P−B_P bonds, whereas the B_E atoms are bonded to the C atoms of the CBC chains. In carbon-rich boron carbide with a composition close to $\sim B_{12}C_3$ (i.e., $\sim B_4C$), extra carbon atoms statistically replace the B_P atoms in the B_{12} cluster,[1,2,12,13] while maintaining the same basic crystal structure of $B_{13}C_2$. Using phonon spectroscopy and theoretical calculations, various other atomic combinations, such as B_9C_3, $B_{10}C_2$ and $B_{11}C$ icosahedra, and CCC, CCB, CBB, BCB, BBB, BVaB (Va means vacancy) and BB_2B chains have also been suggested as possible constituent units of various boron carbide systems.[1,14−17] Although these studies give a detailed picture of the crystal structures and possible disorders in these systems, they have so far not been able to provide a satisfactory explanation of the chemical bonding and the structure−property relationship in boron carbide.[2,17]

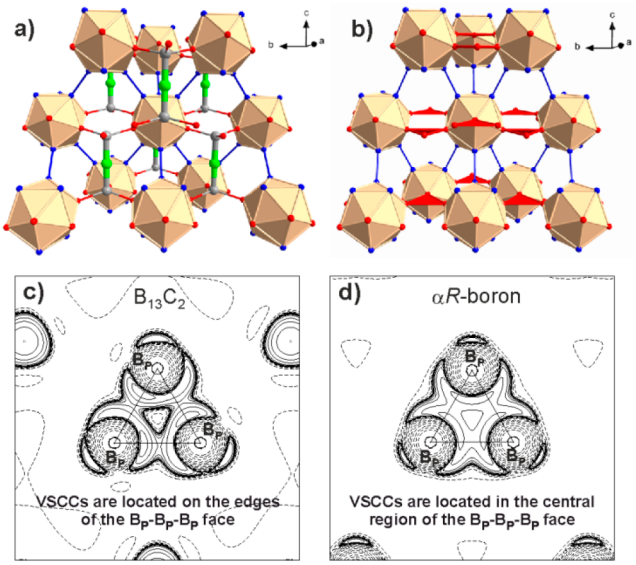

Figure 1. (a) Crystal structure of $B_{13}C_2$. C atoms are drawn in the color gray; B_E, B_P and B_C atoms are drawn in the colors red, blue and green, respectively. The CBC units in $B_{13}C_2$ are drawn with thick bonds. (b) Crystal structures αR-boron with same atom color code as in panel a. Two-electron−three-center (*2e3c*) bonds in αR-boron are shown as red triangles. (c) 6 Å × 6 Å section of the Laplacian in the B_P−B_P−B_P face of the B_{12} cluster in $B_{13}C_2$. Contour lines for the Laplacian are at $\pm(2, 4, 8) \times 10^n$ eÅ^{-5} ($-3 \le n \le 3$) intervals. Locations of valence shell charge concentrations (VSCCs) are mentioned. (d) Same as in panel c in the case of αR-boron.

A quantitative aspherical electron density (ED)[18] study based on high-resolution single-crystal X-ray diffraction data should provide a better understanding of chemical bonding and the structure−property relationship in boron carbide. Recently, we were able to successfully model the ED distribution in stoichiometric $B_{13}C_2$ by multipole (MP) method using the computer program *XD2006*[19] against an extensive single-crystal synchrotron X-ray diffraction data set.[11] The MP model with lattice parameters a = 5.5962(3) Å, c = 12.0661(7) Å yielded an excellent fit to the diffraction data with R_F(obs) = 0.0197, wR_F^2(obs) = 0.0290 [obs. criteria: $I > 3\sigma_I$] (see the Supporting Information (SI)). The composition B6.51(12)C measured by energy dispersive X-ray spectroscopy, together with the best fit of the ordered B_{12}CBC model to the extensive single-crystal X-ray diffraction data set, have provided conclusive evidence for the absence of disorder and defects in the crystal (see SI Section S1).[11] In the previous report on the synthesis of a defects and disorder free single crystal of $B_{13}C_2$,[11] the basic chemical bonding in $B_{13}C_2$ was assumed to be same as in αR-boron, because both materials possess similar structures (Figure 1a,b). However, a subsequent comparative quantitative analysis of the topological and integrated properties of the experimental EDs in $B_{13}C_2$ and in αR-boron[8] now reveals a subtle difference (Tables 1, 2, S1−S5, Figure 1c,d, S1−S3).

Received: May 3, 2017
Published: July 10, 2017

DOI: 10.1021/acs.chemmater.7b02825
Chem. Mater. 2017, 29, 6191−6194

Table 1. Bond Distances and Topological Properties of the Experimental Static EDs for $B_{13}C_2$ (ref 11) and in αR-Boron[8a]

Bond	d (Å)	d_{BCP} (Å)	ρ_{CP} (e/Å^3)	$\nabla^2\rho_{CP}$ (e/Å^5)
Intracluster *2c* bonds, BCPs				
$(B_P-B_P)_{BC}$	1.8053(4)	0.878/0.932	0.736	−0.556
$(B_P-B_P)_{\alpha B}$	1.7555(5)	0.890/0.890	0.820	−2.258
$^{\$}(B_P-B_E)_{BC}$	1.7997(4)	0.972/0.834	0.761	−1.942
$^{\$}(B_P-B_E)_{\alpha B}$	1.8093(5)	0.865/0.946	0.745	−1.388
$^{\#}(B_P-B_E)_{BC}$	1.7848(5)	0.912/0.874	0.802	−1.675
$^{\#}(B_P-B_E)_{\alpha B}$	1.8028(3)	0.858/0.945	0.764	−1.950
$(B_E-B_E)_{BC}$	1.7590(3)	0.886/0.886	0.742	−1.991
$(B_E-B_E)_{\alpha B}$	1.7868(6)	0.894/0.894	0.804	−2.470
Intracluster *3c* bonds, RCPs				
$(B_P-B_P-B_P)_{BC}$	...	...	0.651	0.866
$(B_P-B_P-B_P)_{\alpha B}$	...	...	0.795	−1.155
$(B_P-B_P-B_E)_{BC}$	...	...	0.700	0.200
$(B_P-B_P-B_E)_{\alpha B}$	...	...	0.704	−1.955
$(B_E-B_E-B_P)_{BC}$	...	...	0.711	−0.452
$(B_E-B_E-B_P)_{\alpha B}$	...	...	0.716	−4.321
Intercluster *2c* bonds, BCPs				
$(B_P-B_P)_{BC}$	1.7131(4)	0.857/0.857	1.030	−6.463
$(B_P-B_P)_{\alpha B}$	1.6734(3)	0.837/0.837	1.104	−9.572
Bonds involving CBC unit in $B_{13}C_2$, BCPs				
$(C-B_E)_{BC}$	1.6037(2)	1.082/0.523	1.097	−8.289
$(C-B_C)_{BC}$	1.4324(5)	0.938/0.494	1.556	−8.985
Intercluster *3c* bond in αR-boron, RCP				
$(B_E-B_E-B_E)_{\alpha B}$	...	...	0.557	−1.063

[a] d is the bond-length and d_{BCP} is the distance between BCP and each of the constituent atoms of the bond. Values for $B_{13}C_2$ and αR-boron are indicated by suffixes $_{BC}$ and $_{\alpha B}$ respectively. Prefixes $^{\$}$ and $^{\#}$ indicate two different intracluster B_P-B_E bonds.

Table 2. Volumes (V) of Atomic Basins and Bader Charges (q) of Atoms in $B_{13}C_2$ [ref 11] and in αR-Boron[8] along with Multiplicity (m) in Unit Cell

	$B_{13}C_2$			αR-boron		
Atom	m	V (Å^3)	q (e)	m	V (Å^3)	q (e)
B_P	6	7.808	−0.210	6	4.763	0.067
B_E	6	5.176	0.703	6	5.139	−0.067
B_C	1	1.936	2.298	...	...	...
C	2	14.571	−2.610	...	...	...

The analysis of the topological properties of EDs has been performed with the aid of Bader's quantum theory of atoms in molecules (QTAIM) approach.[18,20] According to the QTAIM approach, a bonding between two atoms is indicated by the existence of a bond critical point (BCP), which is a local minimum (saddle point) in the ED along the bond path between the bonded atoms. Similarly, a ring critical point (RCP) indicates the presence of a ring closed by the bond paths of bonded atoms. Furthermore, values of the ED at BCP or RCP (ρ_{BCP} or ρ_{RCP}) and its Laplacian ($\nabla^2\rho_{BCP}$ or $\nabla^2\rho_{RCP}$) characterize properties of the chemical bonds. For example, a strong covalent bond is indicated by a large value ρ_{BCP} and a large negative value of $\nabla^2\rho_{BCP}$.

The ED from the MP model exhibits BCPs and RCPs for all bonds in $B_{13}C_2$ (Table 1). The existence of BCPs and RCPs for all intracluster bonds indicates the formation of the B_{12} *closo*-cluster in $B_{13}C_2$. It can be seen in Table 1 that ρ_{BCP} and ρ_{RCP} corresponding to 2-center (*2c*) and 3-center (*3c*) bonds of the B_{12} cluster in $B_{13}C_2$ have similar values with the comparable bonds in αR-boron. This indicates that the bonding in the B_{12} *closo*-cluster in $B_{13}C_2$ is predominantly covalent, as in αR-boron.[8] Except for the intracluster B_P-B_P bond, the $\nabla^2\rho_{BCP}$ of all intracluster *2c* bonds have similar values as those observed for αR-boron. The intracluster B_P-B_P bond in $B_{13}C_2$ has a relatively smaller magnitude of $\nabla^2\rho_{BCP}$ than in αR-boron. The $\nabla^2\rho_{RCP}$ corresponding to *3c* bonds of the B_{12} cluster in $B_{13}C_2$ differ drastically from comparable bonds in αR-boron. The difference is largest for the *3c* intracluster $B_P-B_P-B_P$ bond. In fact, $\nabla^2\rho_{RCP}$ corresponding to the *3c* intracluster $B_P-B_P-B_P$ bond in $B_{13}C_2$ has a large positive value, whereas the comparable bond in αR-boron has a large negative value. A positive value of $\nabla^2\rho_{RCP}$ for the *3c* intracluster $B_P-B_P-B_P$ bond can be interpreted using local form of virial theorem as an indication of high kinetic energy density of the electrons associated with this bond.[20] The more delocalized nature of the electrons over the polar region of the icosahedral B_{12} cluster in $B_{13}C_2$ compared to αR-boron is clearly visible in the ED maps (Figures 1c,d, S1−S3).

Among the *exo*-cluster bonds in $B_{13}C_2$ (Table 1), the values of $\nabla^2\rho_{BCP}$ of $C-B_E$ and $C-B_C$ are almost same, but the ρ_{BCP} of $C-B_E$ has a smaller value than the ρ_{BCP} of $C-B_C$. Large negative values of $\nabla^2\rho_{BCP}$ characterize both $C-B_E$ and $C-B_C$ in $B_{13}C_2$ as 2-electron−2-center (*2e2c*) boron−carbon covalent bonds. Comparatively higher value of ρ_{BCP} of $C-B_C$ is probably because of the distribution of valence electrons over a short length due to internal pressure.[11] The elevated nature of the electron density over the $C-B_C$ bond path compared to $C-B_E$ bond path is visible in Figure 2a.

Consideration of the topological properties of the ED together with the bond-lengths (Table 1) in $B_{13}C_2$ leads to an assignment of six *2e2c* $C-B_E$ bonds between the B_{12} cluster and neighboring CBC groups as well as two *2e2c* $C-B_C$ bonds for each CBC chain. This leaves only five electrons per formula unit of $B_{13}C_2$ remaining, forcing the system to make on average six equivalent electron-deficient *5/3e2c* B_P-B_P bonds with the six neighboring clusters of each B_{12} unit (Figure 2b) (see SI Section S2 for detailed electron counting scheme). The claim of *5/3e2c* bonds in the B_P-B_P regions is in agreement with the fact that the bond-length, ρ_{BCP} and $\nabla^2\rho_{BCP}$ of the intercluster B_P-B_P bonds in $B_{13}C_2$ have values that are intermediate between those expected for *2e2c* and *1e2c* intercluster B−B bonds (see SI Section S3).[8,21] The proposal of electron deficient B_P-B_P intercluster bonds in $B_{13}C_2$ is further supported by the fact that the B_{12} cluster is intrinsically electron deficient[2,8] and is known to form unusual and electron deficient bonds.[21] The electron deficient *5/3e2c* intercluster B_P-B_P bond in $B_{13}C_2$ can be understood by invoking resonance structures with contributing *1e2c* and *2e2c* B_P-B_P bonds (Figure 2c). Electrons can thus be redistributed via the delocalized icosahedral B_{12} cluster to achieve the resonance hybrid *5/3e2c* bond in $B_{13}C_2$, somewhat similar to the delocalized π-electron-assisted resonance structure in 2-norbornyl cation.[22] From known bond-lengths of *1e2c* (1.83 Å) and *2e2c* (1.66 Å) bonds,[21] the bond length of the *5/3e2c* resonance hybrid is expected to be close to ∼1.72 Å, which matches well with the observed value of 1.7131(4).

Despite resonance states, the B_{12} cluster in $B_{13}C_2$ contains on average one unpaired electron, which is responsible for the paramagnetism observed in boron carbide.[7] The electron-deficient intercluster B_P-B_P bond also explains why in carbon-rich boron carbide the B_P atoms of the B_{12} cluster are preferentially replaced by carbon atoms (extra electrons) without affecting the basic crystal structure of $B_{13}C_2$.[1,2] Similar kinds of electron deficient intercluster bonds might explain why other

DOI: 10.1021/acs.chemmater.7b02825
Chem. Mater. 2017, 29, 6191−6194

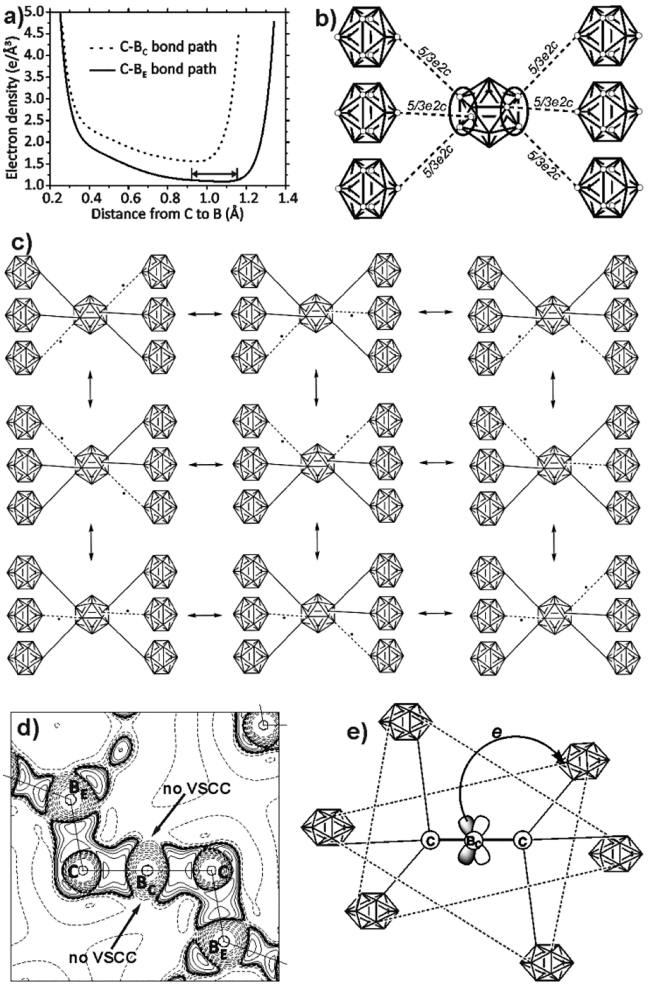

Figure 2. (a) Plot of ED along the C−B_E and C−B_C bond paths. The double arrow indicates the region where the ED remains almost constant along the C−B_E bond path. (b) Resonance hybrid *5/3e2c* intercluster B_P−B_P bonds. B_P atoms are indicated by open circles. The polar region of the central B_{12} cluster has been marked by elliptical lines. (c) Some of the possible contributing structures for the resonance hybrid *5/3e2c* intercluster B_P−B_P bonds. Solid intercluster lines represent *2e2c* intercluster B_P−B_P bonds and dashed lines represent *1e2c* intercluster B_P−B_P bonds. A dot is put beside each *1e2c* bond in order to indicate that they contain single electron. (d) Laplacian of the static ED in the plane containing the atoms B_E, C and B_C [adapted from Figure 2(f) in ref 11]. Contour lines at $\pm(2, 4, 8) \times 10^n$ eÅ^{-3} ($-3 \leq n \leq 3$). (e) Schematic representation of charge transfer from the 2*p* orbitals of the atom B_C to the atom B_P; only one possible charge transfer is shown for clarity.

compounds related to boron carbide such as boron subarsenide ($B_{12}As_2$, intercluster bond-length is ∼1.77 Å), boron subphosphide ($B_{12}P_2$, intercluster bond-length is ∼1.74 Å) can maintain the same general crystal structure over a range of compositions.[13] However, presence of unpaired electrons in $B_{13}C_2$ raises the question as to why $B_{13}C_2$ is chemically stable? The plausible answer is the lack of a possible pathway. Likely causes are steric hindrance and delocalization of the unpaired electrons; both are known to increase the stability of radicals.[23,24] Because of the large number of possible contributing structures (Figure 2c), unpaired electrons in $B_{13}C_2$ are delocalized over a large area, at the same time they are shielded by bulky icosahedral clusters with fully occupied orbitals on their surfaces. These two factors together may make $B_{13}C_2$ a stable radical. In technical boron carbide, the chemical stability may further be increased by the presence of electron-releasing impurities such as carbon. Nevertheless, boron carbide should be highly reactive at high temperature, when available unpaired electrons might gain sufficient energy to overcome the shielding effect. Evidence of high reactivity of boron carbide at elevated temperature has recently been discovered.[25]

From the integrated properties of the electron densities (Table 2), it is found that the volumes of the B_E atomic basins in $B_{13}C_2$ and in αR-boron are almost same, whereas volume of the B_P atomic basin in $B_{13}C_2$ is larger than the same in αR-boron. A large volume of the B_P atomic basin in $B_{13}C_2$ indicates charge accumulation in the B_P atomic basin. Integrated properties of the ED show that different atoms in $B_{13}C_2$ are differently charged. An analysis of the ED distribution along the C−B_E bond-path shows that there exists a length of ∼0.20 Å where the ED is almost constant (Figure 2a). Because of this feature, positions of the BCP and the zero-flux surface[18,20] between the atom C and the atom B_E are dependent on minor variations of the experimental data and thus poorly determinable. Considering this uncertainty as well as the fact that carbon is more electronegative than boron, it can be understood from Table 2 that most part of the large negative charge of the atom C is probably contributed by the three bonded B_E atoms, whereas B_C atom probably contributes a minor part. However, uncertainties in partitioning and the difference between electro-negativities of carbon and boron together cannot alone explain large positive charge of 2.298 *e* of the atom B_C. The large positive charge of the atom B_C thus indicates absence of electrons at the B_C site.

Absence of valence shell charge concentrations in the electron density at the position of the 2*p* orbitals oriented perpendicularly to the CBC unit (Figure 2d) indicates that these orbitals of the atom B_C are empty. A very small volume of the B_C atomic basin indicates that the atom B_C gives away its 2*p* electron. In contrast, it should be noted that the volume of the B_P atomic basin is relatively large and the atom B_P is slightly negatively charged. Because the distribution of ED along the intercluster B_P−B_P bond path is crystallographically symmetric and because there is no difference in electro-negativities between the atom B_P and its neighbors, it is unlikely that there is a buildup of negative charge on the atom B_P unless some charge transfer is taking place. The negative electronic charge of the atom B_P thus indicates that a charge transfer from the atom B_C to the atom B_P occurs. Because the 2*p* orbitals of the atom B_C are empty, it is most likely that the electron is transferred from these orbitals (Figure 2e). The observation of *p*-type excitons at the B_C site in boron carbide[26] supports the claim of the charge-transfer from the 2*p* orbitals of the atom B_C. It is to be expected that transfer of an electron from B_C will be equally distributed over all 6 equivalent B_P atoms of the B_{12} cluster. If this occurs, each B_P atom should have on average a negative charge of ∼1/6*e*, which approximately matches with the Bader charge of the B_P atom (−0.210 *e*). This view is supported by the shape of the B_{12} icosahedron, which is elongated along the crystallographic 3-fold axis of symmetry such that the distances of the B_P atoms to the centroid of the B_{12} icosahedron at 1.725 Å are significantly longer than those of the B_E atoms (1.679 Å). Observations of photocatalytic activity,[5] Seebeck effect[6] and *p*-type excitons[26] in boron carbide suggest that the transfer of charge between the atoms B_C and B_P may occur in both thermal and photo excitations.

In summary, discovery of a new electron-deficient *5/3e2c* intericosahedral B−B bond in stoichiometric boron carbide ($B_{12}CBC$, with $R\bar{3}m$ symmetry) has been reported. It is proposed

DOI: 10.1021/acs.chemmater.7b02825
Chem. Mater. 2017, 29, 6191−6194

that the *5/3e2c* bond is caused by a resonance mechanism with contributing *1e2c* and *2e2c* B−B intericosahedral bonds. The proposed bonding model is consistent with the chemical and physical properties of boron carbide and explains why boron carbide and related materials can preserve the same crystal structure over a range of compositions. This study resolves the long-standing enigma of chemical bonding in boron carbide, and indicates that the properties of boron carbide can be tuned by adjusting the amount of external excitation energy or by changing the chemical composition by bearing the charge distribution in mind. This understanding should have a major impact on designing boron carbide and related materials with improved performance.

■ ASSOCIATED CONTENT

Supporting Information

The Supporting Information is available free of charge on the ACS Publications website at DOI: 10.1021/acs.chemmater.7b02825.

Details of the MP models and the investigations on possible disorder in $B_{13}C_2$; electron counting scheme; summary of the supporting experimental results, comparison of electron density distributions in $B_{13}C_2$ and αR-boron (Figures S1−S3); crystallographic data and parameters from the MP models of $B_{13}C_2$ and αR-boron (Tables S1−S5) and analysis of possible disorder (Table S6) (PDF)

■ AUTHOR INFORMATION

Corresponding Author

*Swastik Mondal. Email: swastik_mondal@cgcri.res.in.

ORCID

Swastik Mondal: 0000-0003-2633-3842

Notes

The author declares no competing financial interest.

■ ACKNOWLEDGMENTS

The author thanks Dr. R. Goddard (Max-Planck-Institut für Kohlenforschung, Kaiser-Wilhelm-Platz 1, 45470 Mülheim an der Ruhr, Germany), Prof. Dr. S. van Smaalen (Laboratory of Crystallography, University of Bayreuth, 95470 Bayreuth, Germany) and Prof. Dr. L. Dubrovinsky (Bayerisches Geoinstitut, University of Bayreuth, 95470 Bayreuth, Germany) for useful discussions and constructive criticism of the present work. The author gratefully acknowledges the support from the Council of Scientific and Industrial Research (CSIR), India.

■ REFERENCES

(1) Domnich, V.; Reynaud, S.; Haber, R. A.; Chhowalla, M. Boron Carbide: Structure, Properties, and Stability under Stress. *J. Am. Ceram. Soc.* **2011**, *94*, 3605−3628.

(2) Balakrishnarajan, M. M.; Pancharatna, P. D.; Hoffmann, R. Structure and Bonding in Boron Carbide: The Invincibility of Imperfections. *New J. Chem.* **2007**, *31*, 473−485.

(3) Thevenot, F. Boron Carbide − a Comprehensive Review. *J. Eur. Ceram. Soc.* **1990**, *6*, 205−225.

(4) Chen, M.; McCauley, J. W.; Hemker, K. J. Shock-induced Localized Amorphization in Boron Carbide. *Science* **2003**, *299*, 1563−1566.

(5) Liu, J.; Wen, S.; Hou, Y.; Zuo, F.; Beran, G. J. O.; Feng, P. Boron Carbides as Efficient, Metal-Free, Visible-Light-Responsive Photocatalysts. *Angew. Chem., Int. Ed.* **2013**, *52*, 3241−3245.

(6) Aselage, T. L.; Emin, D.; McCready, S. S. Conductivities and Seebeck Coefficients of Boron Carbides: Softening Bipolaron Hopping. *Phys. Rev. B: Condens. Matter Mater. Phys.* **2001**, *64*, 054302.

(7) Kakazey, M. G.; Gonzalez-Rodriguez, J. G.; Vlasova, M. V.; Shanina, B. D. Electron Paramagnetic Resonance in Boron Carbide. *J. Appl. Phys.* **2002**, *91*, 4438−4446.

(8) Mondal, S.; van Smaalen, S.; Parakhonskiy, G.; Prathapa, S. J.; Noohinejad, L.; Bykova, E.; Dubrovinskaia, N.; Chernyshov, D.; Dubrovinsky, L. Experimental Evidence of Orbital Order in α-B_{12} and γ-B_{28} Polymorphs of Elemental Boron. *Phys. Rev. B: Condens. Matter Mater. Phys.* **2013**, *88*, 024118.

(9) Yakel, H. L. The Crystal Structure of a Boron-rich Boron Carbide. *Acta Crystallogr., Sect. B: Struct. Crystallogr. Cryst. Chem.* **1975**, *31*, 1797−1806.

(10) Kirfel, A.; Gupta, A.; Will, G. The Nature of the Chemical Bonding in Boron Carbide, $B_{13}C_2$. I. Structure Refinement. *Acta Crystallogr., Sect. B: Struct. Crystallogr. Cryst. Chem.* **1979**, *35*, 1052−1059.

(11) Mondal, S.; Bykova, E.; Dey, S.; Ali, Sk I.; Dubrovinskaia, N.; Dubrovinsky, L.; Parakhonskiy, G.; van Smaalen, S. Disorder and Defects are not Intrinsic to Boron Carbide. *Sci. Rep.* **2016**, *6*, 19330.

(12) Lazzari, R.; Vast, N.; Besson, J. M.; Baroni, S.; Dal Corso, A. Atomic Structure and Vibrational Properties of Icosahedral B_4C Boron Carbide. *Phys. Rev. Lett.* **1999**, *83*, 3230−3033.

(13) *Boron-Rich Solids. AIP Conf. Proc*; Emin, D.; Aselage, T.; Beckel, C. L.; Howard, I. A.; Wood, C., Eds.; American Institute of Physics: New York, 1986; Vol. *140*.

(14) Werheit, H.; Shalamberidze, S. Advanced microstructure of boron carbide. *J. Phys.: Condens. Matter* **2012**, *24*, 385406.

(15) Saal, J. E.; Shang, S.; Liu, Z. The structural evolution of boron carbide via ab initio calculations. *Appl. Phys. Lett.* **2007**, *91*, 231915.

(16) Yao, S.; Gao, Q.; Widom, M. Phase diagram of boron carbide with variable carbon composition. *Phys. Rev. B: Condens. Matter Mater. Phys.* **2017**, *95*, 054101.

(17) Shirai, K.; Sakuma, K.; Uemura, N. Theoretical Study of the Structure of Boron Carbide $B_{13}C_2$. *Phys. Rev. B: Condens. Matter Mater. Phys.* **2014**, *90*, 064109.

(18) Coppens, P. *X-ray Charge Densities and Chemical Bonding*; Oxford University Press: New York, 1997.

(19) Volkov, A.; Macchi, P.; Farrugia, L. J.; Gatti, C.; Mallinson, P.; Richter, T.; Koritsanszky, T. *XD2006, A Computer Program Package for Multipole Refinement, Topological Analysis of Charge Densities and Evaluation of Intermolecular Energies from Experimental or Theoretical Structure Factors*, 2006.

(20) Bader, R. F. W. *Atoms in Molecules - a Quantum Theory*; Oxford University Press: Oxford, U. K., 1990.

(21) Mondal, S.; van Smaalen, S.; Schoenleber, A.; Filinchuk, Y.; Chernyshov, D.; Simak, S. I.; Mikhaylushkin, A. S.; Abrikosov, I. A.; Zarechnaya, E.; Dubrovinsky, L.; Dubrovinskaia, N. Electron Deficient and Polycenter Bonds in the High-Pressure γ-B_{28} Phase of Boron. *Phys. Rev. Lett.* **2011**, *106*, 215502.

(22) Scholz, F.; Himmel, D.; Heinemann, F. W.; Schleyer, P. v. R.; Meyer, K.; Krossing, I. Crystal Structure Determination of the Nonclassical 2-Norbornyl Cation. *Science* **2013**, *341*, 62−64.

(23) Nonhebel, D. C.; Walton, J. C. *Free-Radical Chemistry: Structure and Mechanism*; Cambridge University Press: London, U. K., 1974.

(24) Itoh, T.; Nakata, Y.; Hirai, K.; Tomioka, H. Triplet Diphenylcarbenes Protected by Trifluoromethyl and Bromine Groups. A Triplet Carbene Surviving a Day in Solution at Room Temperature. *J. Am. Chem. Soc.* **2006**, *128*, 957−967.

(25) Sabatini, J. J.; Poret, J. C.; Broad, R. N. Boron Carbide as a Barium-Free Green Light Emitter and Burn-Rate Modifier in Pyrotechnics. *Angew. Chem., Int. Ed.* **2011**, *50*, 4624−4626.

(26) Schmechel, R.; Werheit, H.; Kampen, T. U.; Moench, W. Photoluminescence of Boron Carbide. *J. Solid State Chem.* **2004**, *177*, 566−568.

DOI: 10.1021/acs.chemmater.7b02825
Chem. Mater. 2017, 29, 6191−6194